

Figure S1. Isosurface plots of selected frontier MOs for [Co^{II}(corrin)]⁺ based on uBP86/6-311G(d,p) TD-DFT calculations.

Table S1. The 10 lowest excited states of $[\text{Co}^{\text{II}}(\text{corrin})]^+$, obtained from TD-DFT/BP86/6-311G(d,p) calculations.

| | E(eV) | $\lambda(\text{nm})$ | f | Coeff. | Character | | |
|-----------------|-------|----------------------|--------|--------|---|---|--|
| D ₁ | 0.45 | 2767.4 | 0.0000 | 100 | 94(β) \rightarrow 95(β) | H(β) \rightarrow L(β) | $d_{yz} + \pi \rightarrow d_z^2$ |
| D ₂ | 0.68 | 1834.9 | 0.0000 | 100 | 93(β) \rightarrow 95(β) | H-1(β) \rightarrow L(β) | $d_{xz} + \pi \rightarrow d_z^2$ |
| D ₃ | 1.38 | 898.9 | 0.0007 | 99 | 92(β) \rightarrow 95(β) | H-2(β) \rightarrow L(β) | $d_x^2 - y^2 \rightarrow d_z^2$ |
| D ₄ | 1.52 | 816.6 | 0.0003 | 99 | 91(β) \rightarrow 95(β) | H-3(β) \rightarrow L(β) | $\pi \rightarrow d_z^2$ |
| D ₅ | 1.73 | 716.0 | 0.0005 | 39 | 95(α) \rightarrow 96(α) | H(α) \rightarrow L(α) | $d_{yz} + \pi \rightarrow \pi^*$ |
| | | | | 61 | 94(β) \rightarrow 96(β) | H(β) \rightarrow L+1(β) | $d_{yz} + \pi \rightarrow \pi^*$ |
| D ₆ | 2.13 | 583.3 | 0.0002 | 99 | 90(β) \rightarrow 95(β) | H-4(β) \rightarrow L(β) | $\pi + d_{yz} \rightarrow d_z^2$ |
| | | | | | | H-1(β) \rightarrow L+1(β) | $d_{xz} + \pi \rightarrow \pi^*$ |
| D ₇ | 2.13 | 582.2 | 0.0034 | 8 | 93(β) \rightarrow 96(β) | | |
| | | | | 92 | 94(α) \rightarrow 96(α) | H-1(α) \rightarrow L(α) | $d_{xz} + \pi \rightarrow \pi^*$ |
| | | | | | | H(α) \rightarrow L+1(α) | $\pi \rightarrow \pi^*$ |
| | | | | | | | |
| D ₈ | 2.34 | 529.2 | 0.0002 | 37 | 95(α) \rightarrow 97(α) | | |
| | | | | 15 | 95(α) \rightarrow 97(α) | H(α) \rightarrow L+1(α) | $d_{yz} + \pi \rightarrow d_{xy-n}$ |
| | | | | 38 | 94(β) \rightarrow 98(β) | H(β) \rightarrow L+3(β) | $\pi \rightarrow \pi^*$ |
| | | | | 11 | 94(β) \rightarrow 98(β) | H(β) \rightarrow L+3(β) | $d_{yz} + \pi \rightarrow d_{xy-n}$ |
| D ₉ | 2.37 | 523.9 | 0.0000 | 47 | 95(α) \rightarrow 97(α) | H(α) \rightarrow L+1(α) | $d_{yz} + \pi \rightarrow d_{xy-n}$ |
| | | | | 12 | 95(α) \rightarrow 97(α) | H(α) \rightarrow L+1(α) | $\pi \rightarrow \pi^*$ |
| | | | | 26 | 94(β) \rightarrow 98(β) | H(β) \rightarrow L+3(β) | $d_{yz} + \pi \rightarrow d_{xy-n}$ |
| | | | | 15 | 94(β) \rightarrow 98(β) | H(β) \rightarrow L+3(β) | $\pi \rightarrow \pi^*$ |
| D ₁₀ | 2.38 | 520.8 | 0.0006 | 4 | 95(α) \rightarrow 96(α) | H(α) \rightarrow L(α) | $d_z^2/d_{yz} + \pi \rightarrow \pi^*$ |
| | | | | 96 | 93(β) \rightarrow 97(β) | H-1(β) \rightarrow L+2(β) | $d_x^2 - y^2 \rightarrow \pi^*$ |

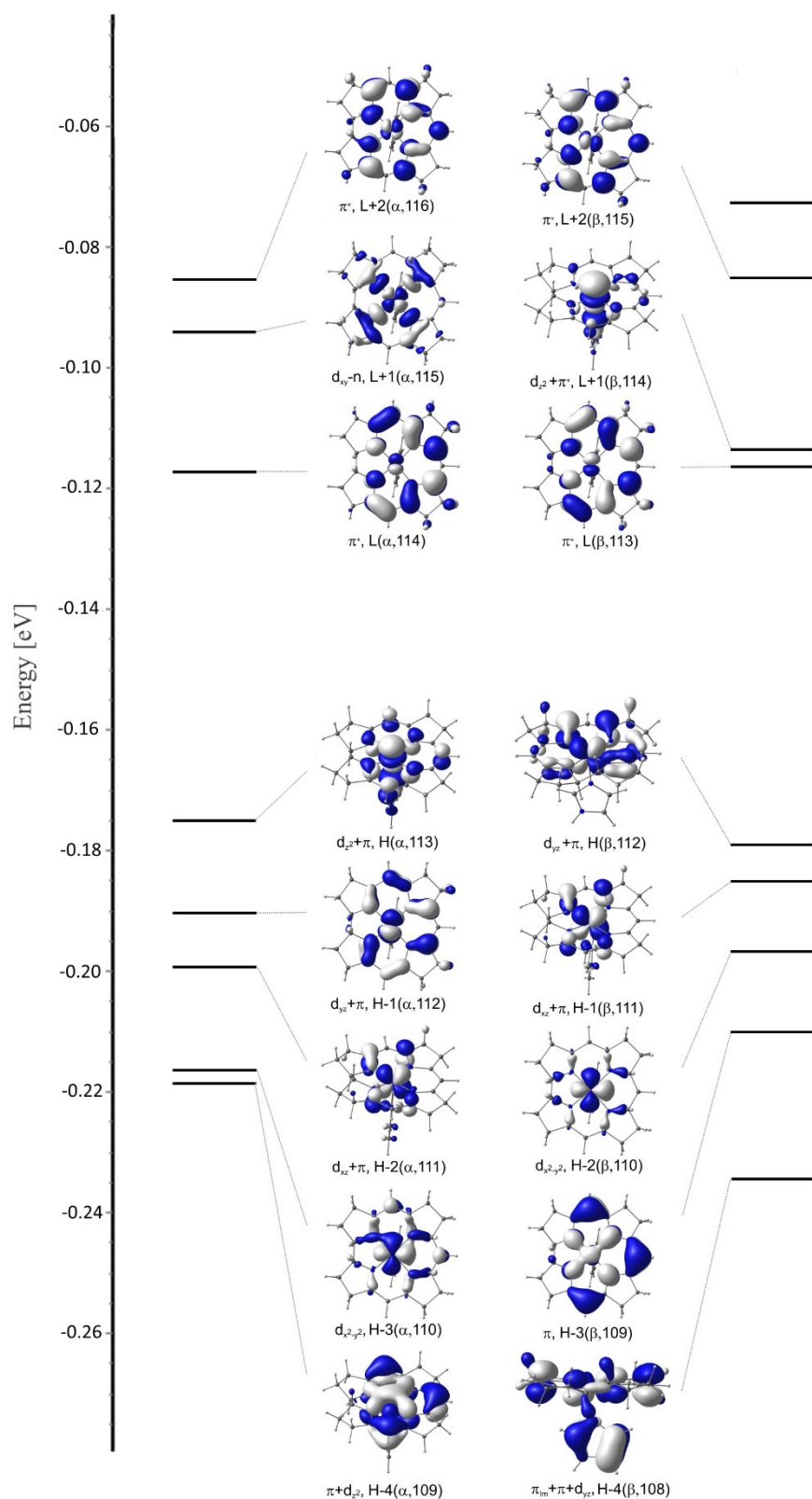


Figure S2. Isosurface plots of selected frontier MOs for [Im-Co^{II}(corrin)]⁺ based on uBP86/6-311G(d,p) calculations .

Table S2 The 10 lowest excited states of [Im-Co^{II}(corrin)]⁺ (2.13 Å min) obtained from TDDFT/BP86/6-311G(d,p) calculations.

| | E(eV) | λ(nm) | <i>f</i> | NTO Coeff. | TDDFT Character | | |
|-----------------|-------|-------|----------|---------------|--------------------|-----------------|--|
| D ₁ | 1.40 | 884.9 | 0.0001 | 31 | 113(α) → 114(α) | H(α) → L(α) | $d_z^2 + \pi_{1m} \rightarrow \pi^*$ |
| | | | | 69 | 112(β) → 114(β) | H(β) → L+1(β) | $d_{yz} + \pi \rightarrow d_z^2 + \pi_{1m}^*$ |
| D ₂ | 1.50 | 826.3 | 0.0008 | 36 | 112(α) → 114(α) | H-1(α) → L(α) | $d_{yz} + \pi \rightarrow \pi^*$ |
| | | | | 64 | 112(β) → 113(β) | H(β) → L(β) | $d_{yz} + \pi \rightarrow \pi^*$ |
| D ₃ | 1.59 | 779.5 | 0.0010 | 17 | 113(α) → 114(α) | H(α) → L(α) | $d_z^2 + \pi_{1m} \rightarrow \pi^*$ |
| | | | | 83 | 111(β) → 113(β) | H-1(β) → L+1(β) | $d_{xz} + \pi \rightarrow d_z^2 + \pi_{1m}^*$ |
| D ₄ | 1.65 | 752.0 | 0.0026 | 52 | 113(α) → 114(α) | H(α) → L(α) | $d_z^2 + \pi_{1m} \rightarrow \pi^*$ |
| | | | | 48 | 112(β) → 114(β) | H(β) → L+1(β) | $d_{yz} + \pi \rightarrow d_z^2 + \pi_{1m}^*$ |
| D ₅ | 1.81 | 683.3 | 0.0028 | 8 | 111(α) → 114(α) | H-2(α) → L(α) | $d_{xz} + \pi_{1m} \rightarrow \pi^*$ |
| | | | | 92 | 111(β) → 113(β) | H-1(β) → L+1(β) | $d_{xz} + \pi_{1m} \rightarrow \pi^*$ |
| D ₆ | 2.13 | 583.6 | 0.0094 | 25 | 112(α) → 114(α) | H-1(α) → L(α) | $d_{yz} + \pi \rightarrow \pi^*$ |
| | | | | 75 | 110(β) → 113(β) | H-2(β) → L+1(β) | $d_{x^2-y^2} + \pi \rightarrow d_z^2 + \pi_{1m}^*$ |
| D ₇ | 2.15 | 576.8 | 0.0045 | 57 | 113(α) → 115(α) | H(α) → L+1(α) | $d_{z^2} + \pi_{1m} \rightarrow d_{xy-n}$ |
| | | | | 34 | 111(α) → 114(α) | H-2(α) → L(α) | $d_{xz} + \pi \rightarrow \pi^*$ |
| | | | | 8 | 110(β) → 113(β) | H-2(β) → L(β) | $d_{x^2-y^2} \rightarrow \pi^*$ |
| D ₈ | 2.17 | 570.5 | 0.0062 | 14 | 112(α) → 114(α) | H-2(α) → L(α) | $d_{yz} + \pi \rightarrow \pi^*$ |
| | | | | 86 | 110(β) → 113(β) | H-2(β) → L(β) | $d_{x^2-y^2} + \pi \rightarrow \pi^*$ |
| D ₉ | 2.22 | 557.6 | 0.0004 | 62 | 112(α) → 115(α) | H-1(α) → L+1(α) | $d_{yz} + \pi \rightarrow d_{xy-n}$ |
| | | | | 38 | 112(β) → 116(β) | H(β) → L+3(β) | $d_{yz} + \pi \rightarrow d_{xy-n}$ |
| D ₁₀ | 2.28 | 543.5 | 0.0026 | 54 | 111(α) → 114(α) | H-2(α) → L(α) | $d_{xz} + \pi \rightarrow \pi^*$ |
| | | | | 33 | 111(α) → 115(α) | H-2(α) → L+1(α) | $d_{xz} + \pi \rightarrow d_{xy-n}$ |
| | | | | 14 | 112(β) → 114(β) | H(β) → L+1(β) | $d_{yz} + \pi \rightarrow d_z^2 + \pi^*$ |

Table S3. Comparison of Co $3d \rightarrow 3d_z^2$ transition energies of $\text{Co}^{\text{II}}(\text{corrin})^+$ obtained from experimental and computed results through MCD spectrum, TDDFT, CASSCF/MC-XQDPT2 and SORCI approaches.

| | donor MO | | |
|-------------------------------|------------------------------------|------------------------------------|-----------------------------------|
| | $3d_{yz}$ | $3d_{xz}$ | $3d_{x^2-y^2}$ |
| MCD expt ^a | < 1.16 eV (9000 cm^{-1}) | < 1.16 eV (9000 cm^{-1}) | 1.68 eV (16500 cm^{-1}) |
| TDDFT(4coord) | 0.45 eV | 0.68 eV | 1.38 eV |
| TDDFT _(LF 5-coord) | 0.72 eV | 0.91 eV | 1.55 eV |
| CASSCF/ MC-XQDPT2 | 0.01 eV | 0.01eV | 1.35 eV |
| SORCI ^a | 0.03 eV (256 cm^{-1}) | 0.26 eV (2154 cm^{-1}) | 1.16 eV (9389 cm^{-1}) |

^a Data from ref. 12.

Table S4. Comparison of Co $3d \rightarrow 3d_{z^2}$ transition energies of $\text{Im}^{-}[\text{Co}^{\text{II}}(\text{corrin})]^+$ obtained from experimental and computed results through MCD spectrum, TDDFT, CASSCF/XMCQDPT2 and SORCI approaches.

| | donor MO | | |
|---------------------------|----------------------------------|----------------------------------|-----------------------------------|
| | $3d_{yz}$ | $3d_{xz}$ | $3d_{x^2-y^2}$ |
| MCD expt ^a | 1.79 eV (14470cm ⁻¹) | 1.79 eV (14470cm ⁻¹) | 2.19 eV (17700 cm ⁻¹) |
| TDDFT _(trunc.) | 1.40 eV | 1.59 eV | 2.13 eV |
| TDDFT _(full) | 1.27 eV | 1.42 eV | 2.08 eV |
| TDDFT _(LF) | 0.72 eV | 0.91 eV | 1.55 eV |
| CASSCF/ XMCQDPT2 | 0.90 eV | 0.90 eV | 2.09 eV |

^a read from ref. 24.

Table S5. The 10 lowest excited states [Im-Co^{II}(corrin)]⁺ (1.85 Å) obtained from TDDFT/BP86/6-311G(d,p) calculations.

| | E(eV) | λ(nm) | <i>f</i> | Coeff. | TDDFT Character | | |
|-----------------|-------|--------|----------|--------|-----------------|-----------------|---|
| D ₁ | 0.83 | 1495.1 | 0.0007 | 99 | 112(α) → 113(α) | H-2(α) → L(α) | $d_z^2 + \pi_{1m} \rightarrow \pi^*$ |
| | | | | 1 | 91(β) → 96(β) | H-3(β) → L+1(β) | $d_{yz} + \pi \rightarrow d_z^2 + \pi_{1m}^*$ |
| D ₂ | 1.50 | 829.3 | 0.0004 | 34 | 93(α) → 96(α) | H-2(α) → L(α) | $\pi \rightarrow \pi^*$ |
| | | | | 66 | 91(β) → 96(β) | H-3(β) → L+1(β) | $\pi \rightarrow \pi^*$ |
| D ₃ | 1.54 | 805.7 | 0.0016 | 92 | 93(α) → 96(α) | H-2(α) → L(α) | $d_z^2 + \pi_{1m} \rightarrow d_{xy-n}$ |
| | | | | 8 | 91(β) → 96(β) | H-3(β) → L+1(β) | $d_{yx} + \pi \rightarrow \pi^*$ |
| D ₄ | 1.69 | 731.9 | 0.0005 | 92 | 93(α) → 96(α) | H-2(α) → L(α) | $d_z^2 + \pi_{1m} \rightarrow \pi^*$ |
| | | | | 8 | 91(β) → 96(β) | H-3(β) → L+1(β) | $d_{yz} + \pi + \pi_{1m} \rightarrow d_z^2 + \pi$ |
| D ₅ | 1.77 | 699.3 | 0.0018 | 11 | 93(α) → 96(α) | H-2(α) → L(α) | $d_{xz} + \pi + \pi_{1m} \rightarrow \pi^*$ |
| | | | | 89 | 91(β) → 96(β) | H-3(β) → L+1(β) | $d_{xz} + \pi + \pi_{1m} \rightarrow \pi^*$ |
| D ₆ | 2.04 | 608.1 | 0.0007 | 6 | 93(α) → 96(α) | H-2(α) → L(α) | $d_{xz} + \pi + \pi_{1m} \rightarrow \pi^*$ |
| | | | | 94 | 91(β) → 96(β) | H-3(β) → L+1(β) | $d_{yx} + \pi \rightarrow d_z^2 + \pi$ |
| D ₇ | 2.14 | 578.6 | 0.0041 | 60 | 93(α) → 96(α) | H-2(α) → L(α) | $d_{xz} + \pi + \pi_{1m} \rightarrow \pi^*$ |
| | | | | 40 | 91(β) → 96(β) | H-3(β) → L+1(β) | $d_z^2 / d_{yz} + \pi + \pi_{1m} \rightarrow d_z^2 + \pi$ |
| D ₈ | 2.16 | 574.9 | 0.0031 | 28 | 93(α) → 96(α) | H-2(α) → L(α) | $d_{xz} + \pi + \pi_{1m} \rightarrow \pi^*$ |
| | | | | 72 | 91(β) → 96(β) | H-3(β) → L+1(β) | $d_x^2 - y^2 \rightarrow \pi^*$ |
| D ₉ | 2.18 | 568.7 | 0.0061 | 8 | 93(α) → 96(α) | H-2(α) → L(α) | $d_{yx} + \pi \rightarrow \pi^*$ |
| | | | | 68 | 91(β) → 96(β) | H-3(β) → L+1(β) | $d_{yx} + \pi \rightarrow d_z^2 + \pi_{1m}$ |
| D ₁₀ | 2.24 | 553.0 | 0.0044 | 24 | 91(β) → 96(β) | H-3(β) → L+1(β) | $d_x^2 - y^2 \rightarrow \pi^*$ |
| | | | | 61 | 93(α) → 96(α) | H-2(α) → L(α) | $d_{yx} + \pi \rightarrow d_{xy-n}$ |
| | | | | 39 | 91(β) → 96(β) | H-3(β) → L+1(β) | $d_{yx} + \pi \rightarrow d_{xy-n}$ |

Figure S3. NTOs for [Im-Co^{II}(corrin)]⁺ (1.85 Å)

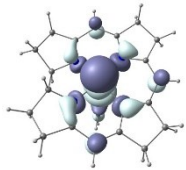
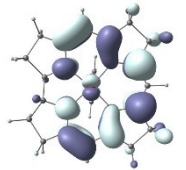
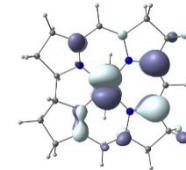
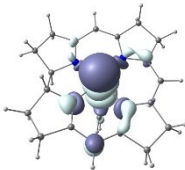
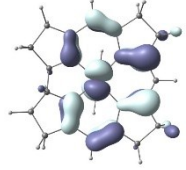
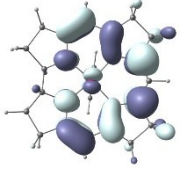
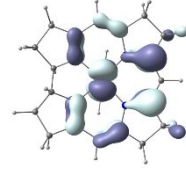
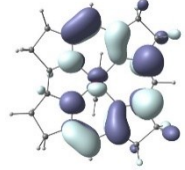
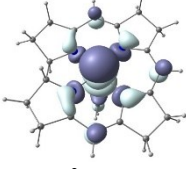
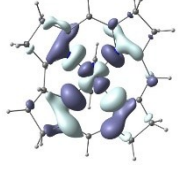
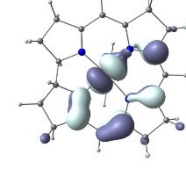
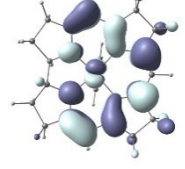
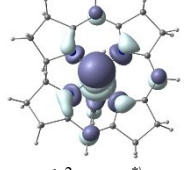
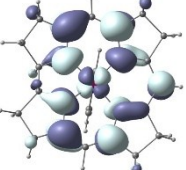
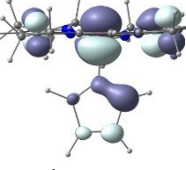
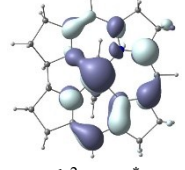
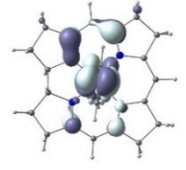
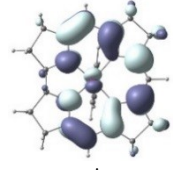
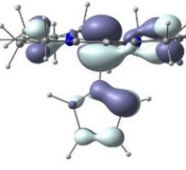
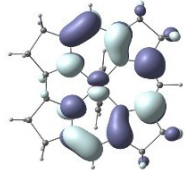
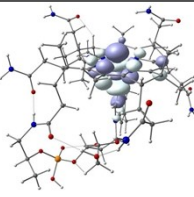
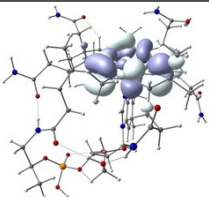
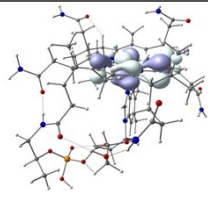
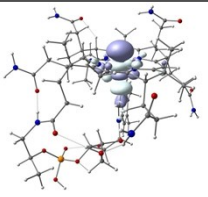
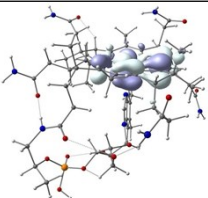
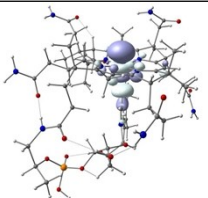
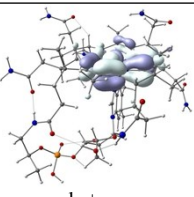
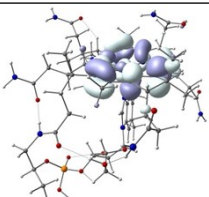
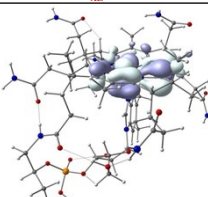
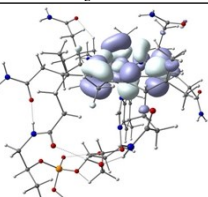
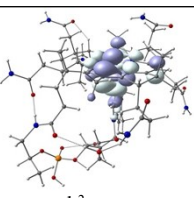
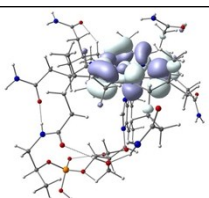
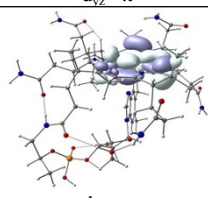
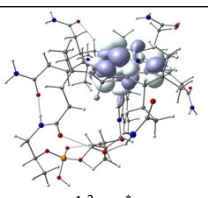
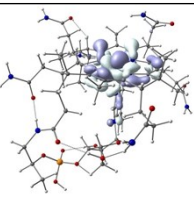
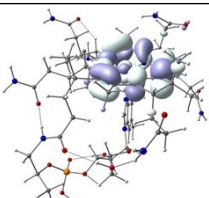
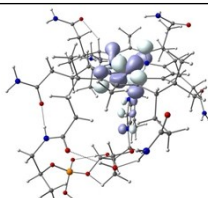
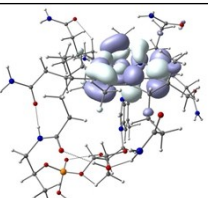
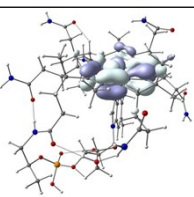
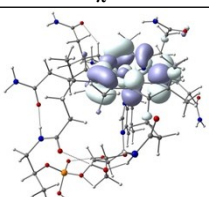
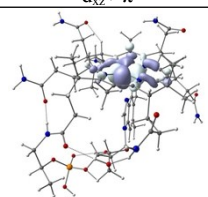
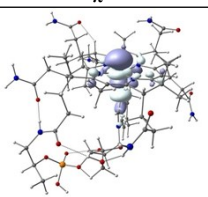
| NTO | E(eV) | NTO Coeff | f | α hole | α particle | β hole | β particle |
|----------------|-------|-----------------------------------|--------|--|--|--|--|
| D ₁ | 0.83 | 99 (α) 1 (β) | 0.0007 |  $d_z^2 + \pi_{1m}$ |  π^* |  $d_{yz} + \pi$ |  $d_z^2 + \pi_{1m}^*$ |
| D ₂ | 1.50 | 34 (α) 66 (β) | 0.0004 |  π |  π^* |  π |  π^* |
| D ₃ | 1.54 | 92 (α) 8 (β) | 0.0016 |  $d_z^2 + \pi_{1m}$ |  $d_{xy}-n$ |  $d_{yx} + \pi$ |  π^* |
| D ₄ | 1.69 | 92 (α) 8 (β) | 0.0005 |  $d_z^2 + \pi_{1m}^*$ |  π^* |  $d_{yz} + \pi + \pi_{1m}$ |  $d_z^2 + \pi_{1m}^*$ |
| D ₅ | 1.77 | 11 (α) 89 (β) | 0.0018 |  $d_{xz} + \pi + \pi_{1m}$ |  π^* |  $d_{xz} + \pi + \pi_{1m}$ |  π^* |

Figure S4. NTOs of the first 10 TDDFT excited states of the $[\text{Im-Co}^{\text{II}}(\text{corrin})]^+$ full structure at the BP86/6-311G (d,p) level of theory.

| NTO | eV | NTO Coeff. & TDDFT Character | f | α hole | α particle | β hole | β particle |
|----------------|------|---|--------|--|---|---|--|
| D ₁ | 1.27 | 6%(α) H \rightarrow L 94 %(β) H \rightarrow L | 0.0001 |  $d_z^2 + \pi_{\text{Im}}$ |  π^* |  $d_{yz} + \pi$ |  $d_z^2 + \pi$ |
| D ₂ | 1.42 | 100 %(β) H-1 \rightarrow L | 0.0001 | | |  $d_{xz} + \pi$ |  $d_z^2 + \pi$ |
| D ₃ | 1.48 | 37% (α) H-1 \rightarrow L 63% (β) H \rightarrow L+1 | 0.0005 |  $d_{yz} + \pi_{\text{Im}}$ |  π^* |  $d_{yz} + \pi$ |  π^* |
| D ₄ | 1.72 | 91% (α) H \rightarrow L 8% (β) | 0.0074 |  $d_z^2 + \pi_{\text{Im}}$ |  π^* |  $d_{yz} + \pi$ |  $d_z^2 + \pi^*$ |
| D ₅ | 1.78 | 14 % (α) H-2 \rightarrow L 85 % (β) H-2 \rightarrow L+1 | 0.0023 |  $d_{xz} + \pi$ |  π^* |  $d_{xz} + \pi$ |  π^* |
| D ₆ | 2.00 | 14% (α) H-1 \rightarrow L 86 % (β) H-2 \rightarrow L | 0.0079 |  $d_{yz} + \pi$ |  π^* |  $d_{x^2-y^2}$ |  d_z^2 |

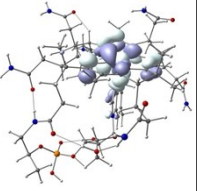
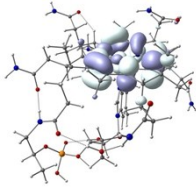
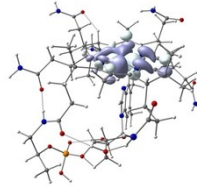
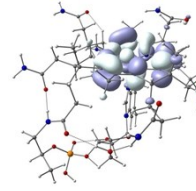
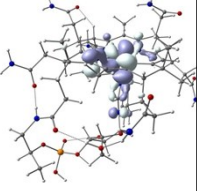
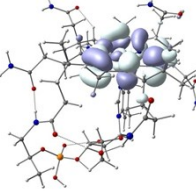
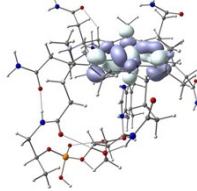
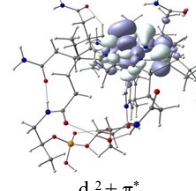
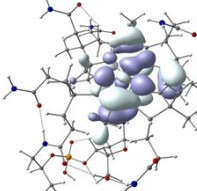
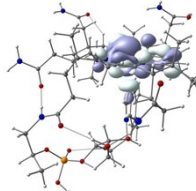
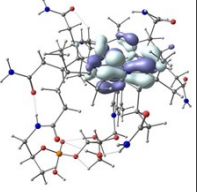
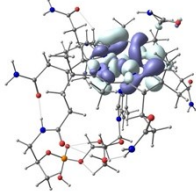
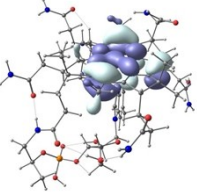
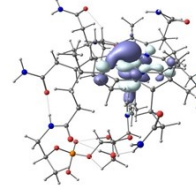
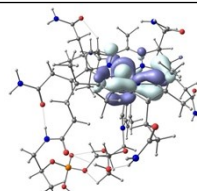
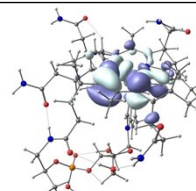
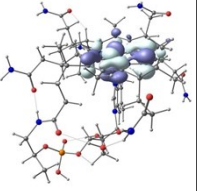
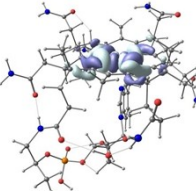
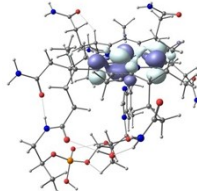
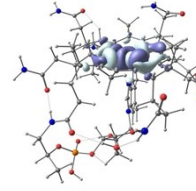
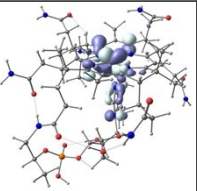
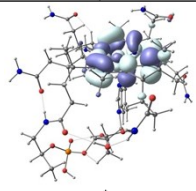
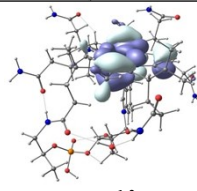
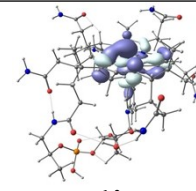
| | | | | | | | |
|-----------------|------|--|--------|---|--|---|---|
| D ₇ | 2.08 | 11% (α) H-3→L 89% (β) H-2 → L+1 *H-3= $\pi + d_z^2$ | 0.0027 |  $d_{yz} + \pi$ |  π^* |  $d_{x^2-y^2} + \pi$ |  $\pi^* + d_z^2$ |
| D ₈ | 2.15 | 60% (α) H-2→L 25% (β 1) 16% (β 2) | 0.0080 |  $d_{xz} + \pi$ |  π^* |  $d_{x^2-y^2} + d_{yz} + \pi$ |  $d_z^2 + \pi^*$ |
| | | | | | |  π |  d_z^2 |
| D ₉ | 2.18 | 40% (α) H-1→L+1 35% (β 1) H-3→L 24% (β 2) | 0.0064 |  $d_{yz} + \pi$ |  $d_{xy}-n$ |  $+ d_z^2$ |  π d_z^2 |
| | | | | | |  $d_z^2 + d_{yz} + \pi$ |  $d_{xy}-n + \pi^*$ |
| D ₁₀ | 2.23 | 36% (α 1) H-1→L+1 26% (α 2) H-2→L 22% (β 1) H→L+4 14% (β 2) H-3→L | 0.0018 |  $d_{yz} + \pi$ |  $d_{xy}-n$ |  $d_{yz} + \pi$ |  $d_{xy}-n$ |
| | | | |  $d_{yz} + \pi$ |  π^* |  $\pi + d_z^2$ |  d_z^2 |

Figure S5. Frontier orbitals of the cob(II)alamin full structure at the BP86/6-311G(d,p) level (left panel), and the BP86/SDD level (right panel).

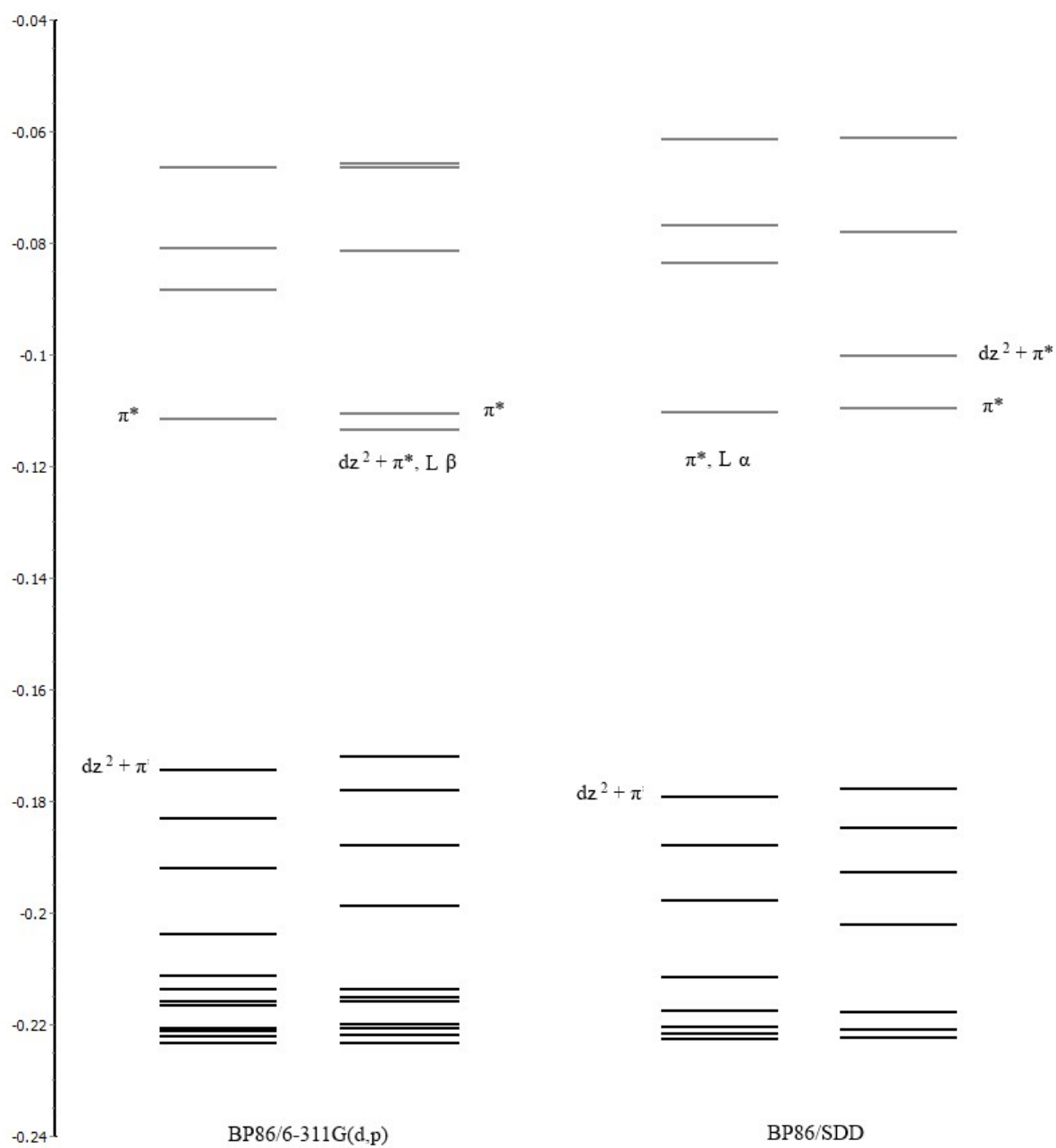


Figure S6. Frontier orbitals of the cob(II)alamin full structure at the BP86/SDD level of theory.

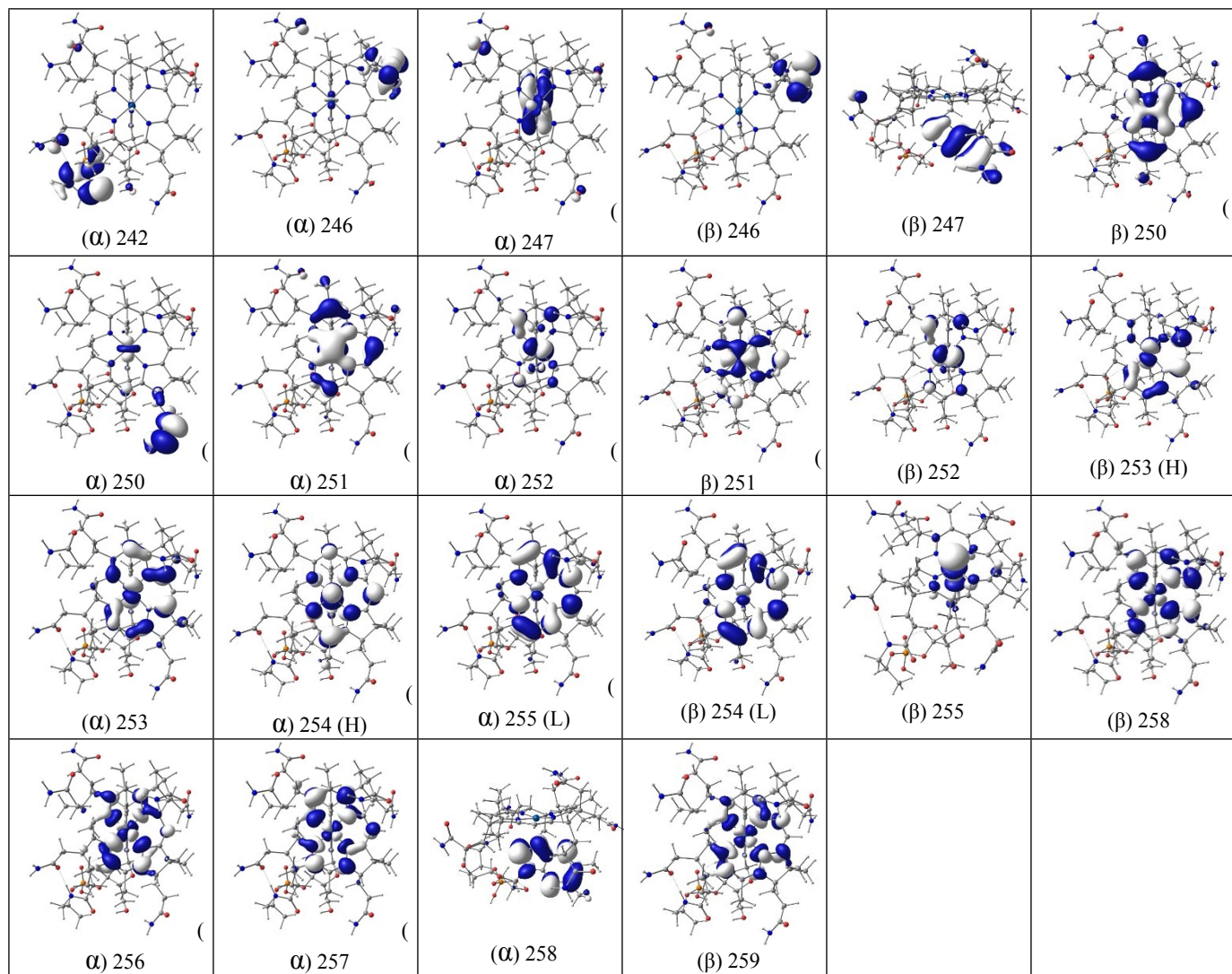


Figure S7. NTOs of the first 5 TDDFT excited states of cob(II)alamin at the BP86/SDD level of theory.

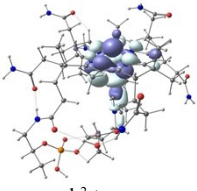
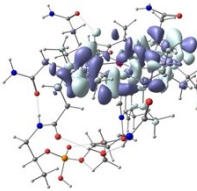
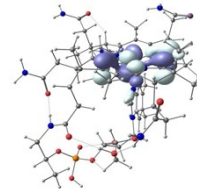
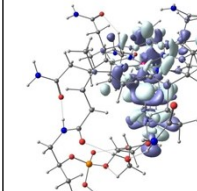
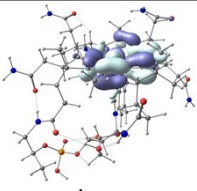
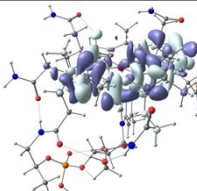
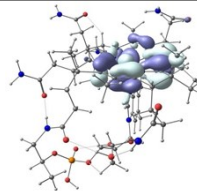
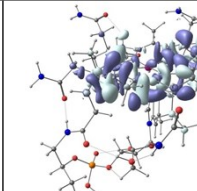
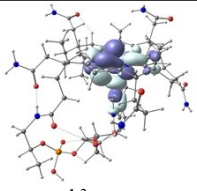
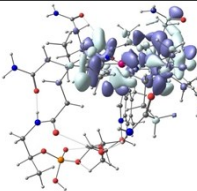
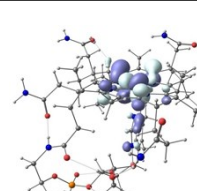
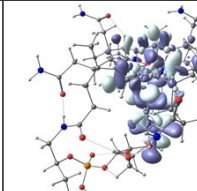
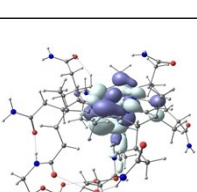
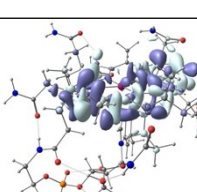
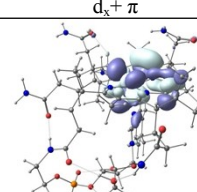
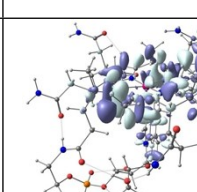
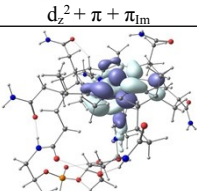
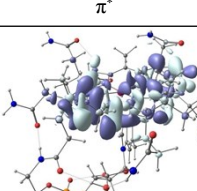
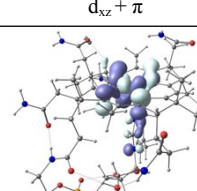
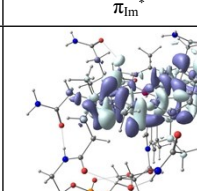
| NTO | eV | NTO Coeff | f | α hole | α particle | β hole | β particle |
|----------------|------|-------------------------------------|--------|--|---|---|---|
| D ₁ | 1.37 | 93% (β) 7% (α) | 0.0001 |  $d_z^2 + \pi_{1m}$ |  π^* |  $d_{yz} + \pi$ |  $d_z^2 + \pi_{1m}$ |
| D ₂ | 1.46 | 62% (β) 38% (α) | 0.0001 |  $d_{yz} + \pi$ |  π^* |  $d_{yz} + \pi$ |  π^* |
| D ₃ | 1.53 | 96% (β) 4% (α) | 0.0005 |  $d_z^2 + \pi_{1m}$ |  π^* |  $d_x + \pi$ |  $d_z^2 + \pi^*$ |
| D ₄ | 1.76 | 80% (α) 20% (β) | 0.0074 |  $d_z^2 + \pi + \pi_{1m}$ |  π^* |  $d_{xz} + \pi$ |  π_{1m}^* |
| D ₅ | 1.84 | 80% (α) 20% (β) | 0.0023 |  $d_z^2 + d_{xz} + \pi_{1m}$ |  π^* |  $d_{xz} + \pi$ |  π^* |

Figure S8. NTOs of selected TDDFT excited states of the cob(II)alamin full structure at the BP86/SDD (d,p) level of theory.

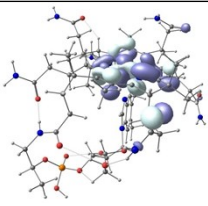
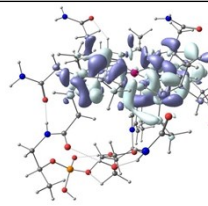
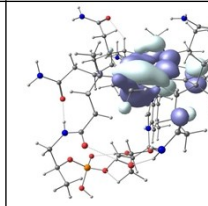
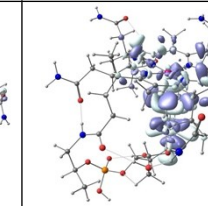
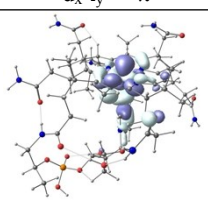
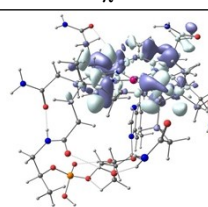
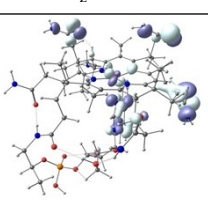
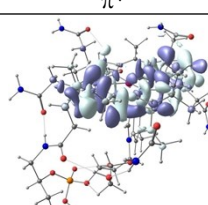
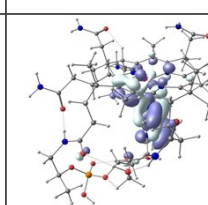
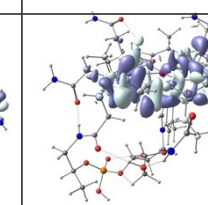
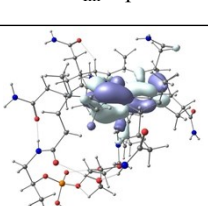
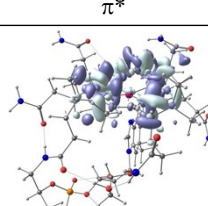
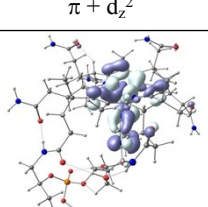
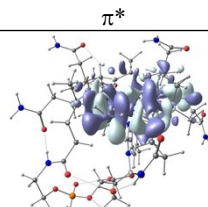
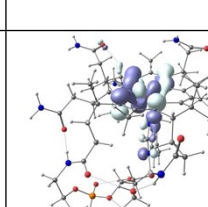
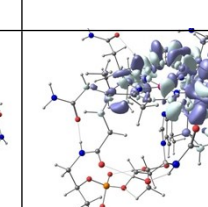
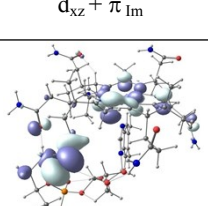
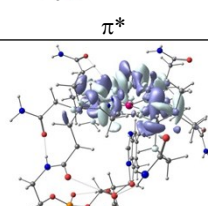
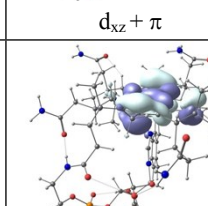
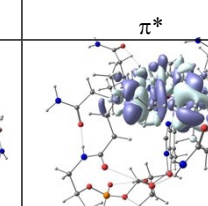
| NTO | eV | NTO Coeff. | f | α hole | α particle | β hole | β particle |
|------------------|------|---|--------|--|---|--|---|
| D ₁₉ | 2.71 | 46% ($\alpha,1$) 29% ($\beta,1$) | 0.0276 |  $d_{x^2-y^2} + \pi$ |  π^* |  $d_{x^2-y^2} + \pi$ |  $d_{z^2} + \pi_{1m}^*$ |
| | | 25% ($\alpha,2$) | |  $d_z^2 + \pi$ |  π^* | | |
| D ₂₉ | 2.93 | 63% ($\alpha,1$) 19% ($\beta,1$) | 0.0377 |  $\pi_{1m} + p$ |  π^* |  π_{1m} |  π^* |
| | | 19% ($\alpha,2$) | |  $\pi + d_z^2$ |  π^* | | |
| D ₆₁ | 3.39 | 78% (β) 22% (α) | 0.0263 |  $d_{xz} + \pi_{1m}$ |  π^* |  $d_{xz} + \pi$ |  π^* |
| D ₁₄₄ | 3.95 | 60% (β) 40% (α) | 0.0923 |  π_p |  π^* |  $d_{x^2-y^2} + \pi$ |  d_{xy-n} |

Figure S9. NTOs of selected TDDFT excited states of the $[\text{Im-Co}^{\text{II}}(\text{corrin})]^+$ (min, 2.13 Å) model at the BP86/6-311g (d,p) level of theory.

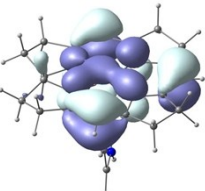
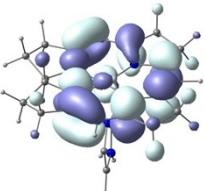
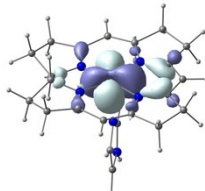
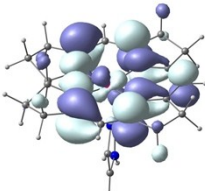
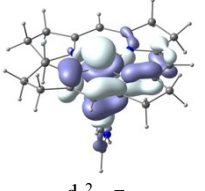
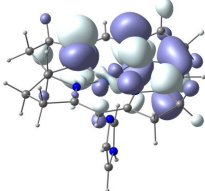
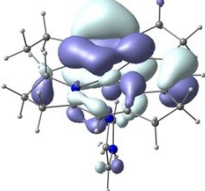
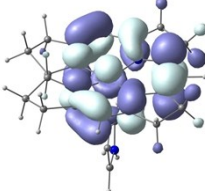
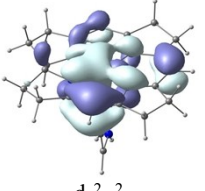
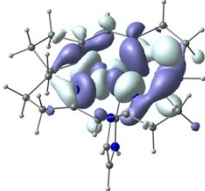
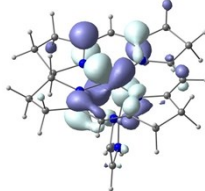
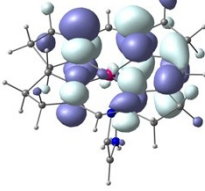
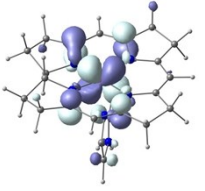
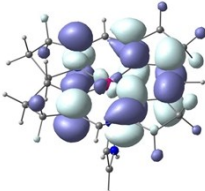
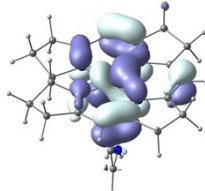
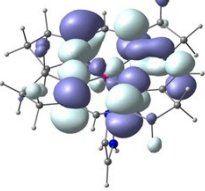
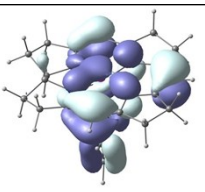
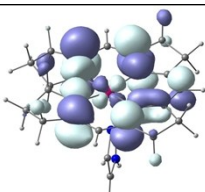
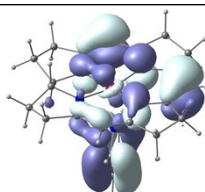
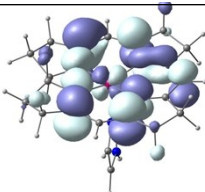
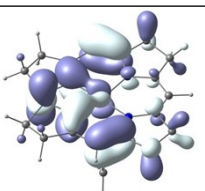
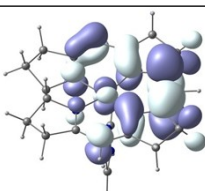
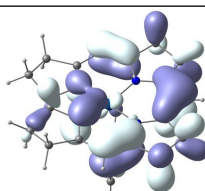
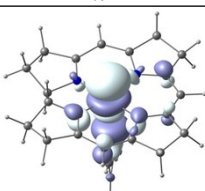
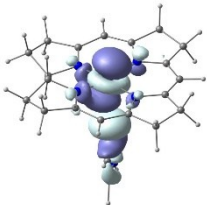
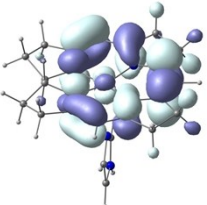
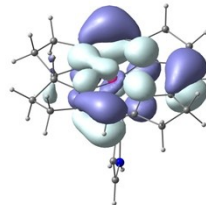
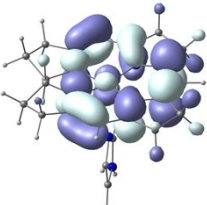
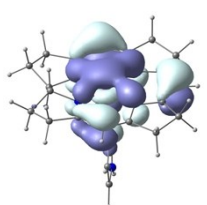
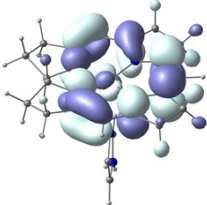
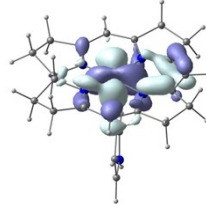
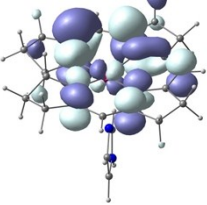
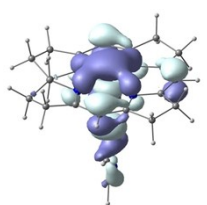
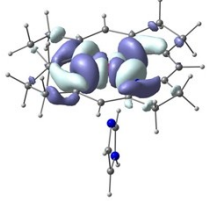
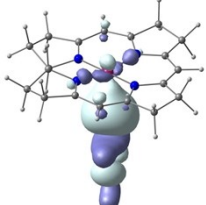
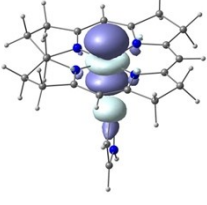
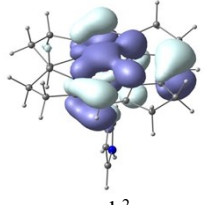
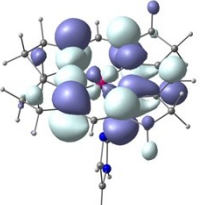
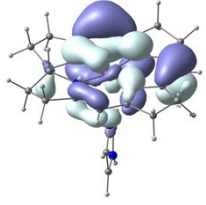
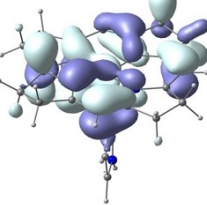
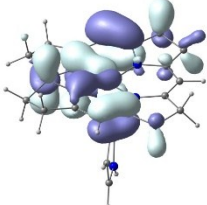
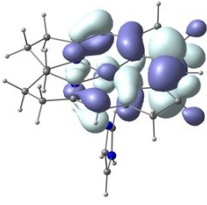
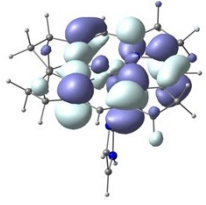
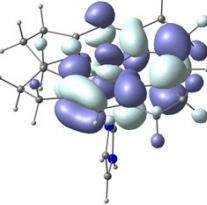
| NTO | eV | NTO Coeff. | f | α hole | α particle | β hole | β particle |
|-----------------|------|---|--------|---|---|--|--|
| D ₂₃ | 3.00 | 32 % ($\alpha,1$) 30 % ($\beta,1$) | 0.0160 |  $\pi + d_z^2$ |  π^* |  $d_{x^2-y^2}$ |  d_{xy-n} |
| | | 17 % ($\alpha,2$) 30 % ($\beta,2$) | |  $d_z^2 + \pi$ |  π^* |  π |  $d_{z^2} + \pi^*$ |
| D ₃₃ | 3.38 | 75 % (β) 25 % (α) | 0.0500 |  $d_{x^2-y^2}$ |  d_{xy-n} |  $d_{xz} + \pi$ |  π^* |
| D ₄₅ | 3.80 | 89 % (α) 11 % (β) | 0.0689 |  $d_{xz} + \pi + \pi_{\text{Im}}$ |  π^* |  $d_{xz} + \pi$ |  π^* |
| D ₅₆ | 4.09 | 37 % ($\alpha,1$) 33 % ($\beta,1$) | 0.2433 |  $\pi + \pi_{\text{Im}} + d_z^2$ |  π^* |  $\pi + \pi_{\text{Im}} + d_z^2$ |  π^* |
| | | 13 % ($\alpha,2$) 18 % ($\beta,2$) | |  π |  π^* |  π |  d_z^2 |

Figure S10. NTOs of selected TDDFT excited states of the [Im- - Co^{II}(corrin)]⁺_(LF, 2.80 Å) model at the BP86/6-311g (d,p) level of theory.

| NTO | eV | NTO Coeff. | <i>f</i> | α hole | α particle | β hole | β particle |
|-----------------|------|---|----------|---|---|--|--|
| D ₁₇ | 2.73 | 58 % (α) 42 % (β) | 0.0455 |  $d_z^2 + \pi$ |  π^* |  $d_z^2 + \pi$ |  π^* |
| D ₂₆ | 3.09 | 66 % (α) 34 % (β) | 0.0953 |  $\pi + d_z^2$ |  π^* |  $d_{x^2-y^2}$ |  π^* |
| D ₃₃ | 3.44 | 74 % (β) 26 % (α) | 0.0520 |  $\pi + d_z^2$ |  $d_{xy}-n$ |  π |  $d_z^2 + \pi_{Im}^*$ |
| D ₅₄ | 4.06 | 40 % ($\alpha,1$) 33 % ($\beta,1$) | 0.2472 |  $\pi + d_z^2$ |  π |  π |  π^* |
| | | 15 % ($\alpha,2$) 12 % ($\beta,2$) | |  $\pi + d_{yz}$ |  π^* |  π |  $d_{yz} + \pi^*$ |